Broadband noise investigation on rod-airfoil-configurations

J. Giesler, E. Sarradj
Brandenburg University of Technology, Aeroacoustics Group, Cottbus, Germany
Email: jens.giesler@tu-cottbus.de / ennes.sarradj@tu-cottbus.de

Introduction

One important broadband noise generating mechanism in axial-flow compressors is the interaction between the turbulent inflow or a turbulent wake of a rotor blade and the leading edge (LE) of the downstream stator blade. Additionally, the interaction of turbulent vortices and the trailing edge (TE) of the airfoil generates noise as well. These mechanism are investigated in a research project at the Brandenburg University of Technology. To analyze broadband noise emission a test setup is installed in the aeroacoustic wind tunnel [1, 2] which basically consists of a rod-airfoil-configuration. This configuration is suited to model noise generating mechanisms like turbulent inflow to blades and stator-rotor interactions. A similar setup has been used by Jacob et al. [3] for the verification of numeric broadband noise calculations. In this project the broadband noise is investigated for different setup configurations using a microphone array, wall pressure sensors and hotwire anemometry.
The paper explains the experimental setup and gives details on the measurement procedure. First acoustic results are discussed.

Experimental setup

A schema of the experimental setup is shown in Figure 1. It consists of a rod and an airfoil mounted downstream of the rod. The test setup allows the variation of the flow speed, the airfoil geometry, the rod diameter and the distance between cylinder and the leading edge of the airfoil.

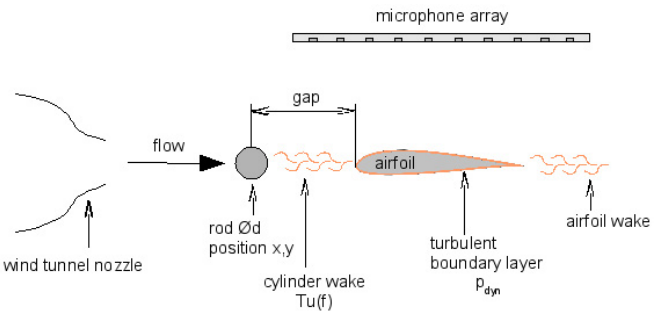

Figure 1: Schema of the experimental setup.

The flow speed is adjusted in 27 steps between 26 m/s and 72 m/s giving a Mach number range from 0.08 to 0.21. Airfoils of NACA 0012 and NACA 0018 type with a chord length of 100 mm and a span width of 120 mm are used. By changing the rod diameter and the gap between rod and the leading edge of the airfoil the airfoil inflow characteristic is varied. The diameters of the rods that were used are 5 mm, 7 mm, 10 mm, 13 mm and 16 mm and the gaps can be adjusted 86 mm, 96 mm, 106 mm, 113 mm and 124 mm. A total of 50 configurations have been tested. To enable a better flow quality and to minimize background noise the rod-airfoil-configuration is mounted between two parallel sound absorbing side plates directly attached to the rectangular nozzle exit. A picture of the rod-airfoil-configuration mounted in the measurement area of the wind tunnel is shown in Figure 2.

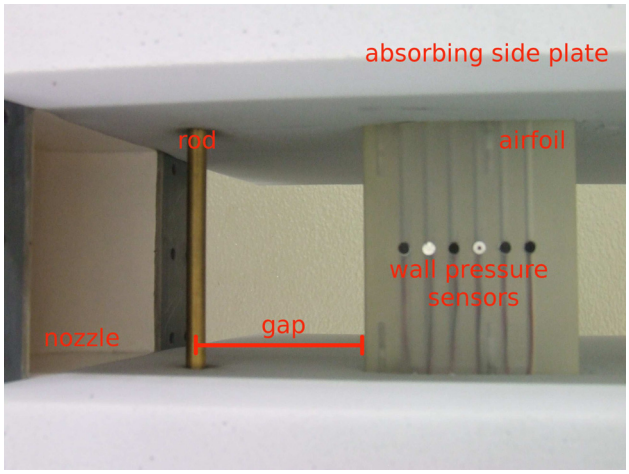

Figure 2: Rod-airfoil-configuration mounted between two absorbing side plates directly attached to the wind tunnel nozzle exit. The installed airfoil has flush integrated dynamic wall pressure sensors.

To separate the different noise source locations (rod, LE, TE) and to eliminate background noise influences the radiated sound is measured using a flush mounted 38-channel microphone array. The array is installed 0.721 m above the rod-airfoil plane and has an aperture of 1.4 m x 0.4 m.
For the turbulent boundary layer noise generating mechanism the dynamic wall pressure fluctuations and their propagation over the airfoil surface are important parameters. Therefore, these fluctuations are measured by six small electret microphone capsules. The capsules are integrated into the airfoil in the chord direction.
The turbulence intensities and the turbulent length scales at the LE are important parameters for the LE noise generating mechanism. They have been quantified in a separate hotwire measurement series using a single Dantec 55P11 hotwire probe.

Data analysis

The microphone array data and the data of the wall pressure sensors are captured simultaneously by a multi channel A/D unit connected to a PC. A sample rate of

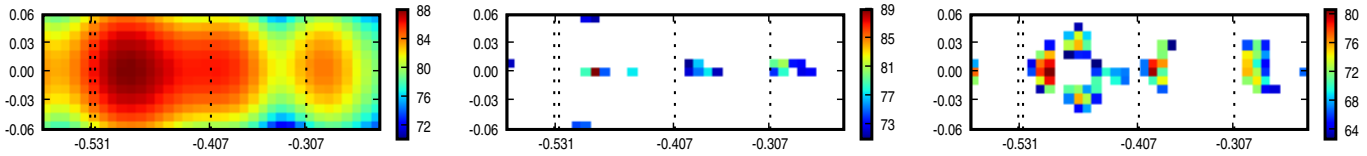

(a) Delay and sum bf (b) Orthogonal bf, 16 eigenvalues (c) DAMAS bf, 500 iterations

Figure 3: Comparison of the spatial resolution of different beamforming (bf) algorithms on a rod-airfoil-configuration. Shown are pictures for a flow speed of 72 m/s and the 5 kHz third octave band (flow from left to right).

51200 Hz and a measurement time of 40 seconds are used for capturing. After recording the acoustic data are processed by various beamforming algorithms. The result of the beamforming process is a two dimensional image of the acoustic source distribution, in the following referred to as sound map. To compare the noise emission at the rod, the LE and the TE, different sectors are defined corresponding to those segments. Then the beamforming result is integrated over these sectors to obtain a frequency spectrum characterizing the noise emission for each sector.

To choose an algorithm particularly suitable to separate the different noise source locations (rod, LE, TE), delay and sum beamforming, orthogonal beamforming [4] using 16 eigenvalues and DAMAS (deconvolution approach for the mapping of acoustic sources) [5] with 500 iterations were tested for two configurations. In Figure 3 the sound maps for the configuration composed of the 5 mm rod, a gap of 124 mm and the NACA 0018 airfoil are shown for the different beamforming algorithms. Because of the relatively good spatial resolution of the DAMAS sound map, DAMAS is chosen for further analyses. It should be noted that according to Sarradj [6] DAMAS has some difficulties with the weak TE noise source of the rod-airfoil-configuration. Therefore orthogonal beamforming will be used additionally in future.

Because broadband noise is the point of interest the influence of the tonal characteristics of the cylinder wake (aeolian cylinder tones) has to be excluded. The calculated aeolian tone for the configurations with a rod of 5 mm is 2880 Hz. Thus, the noise emission is analyzed for third octave bands with center frequencies equal to or greater than 4 kHz.

The present paper focusses on acoustical analysis and omits the results of the wall pressure and the hotwire data.

Results

To investigate the broadband noise emission for different rod-airfoil-configurations various spectra are analyzed. All spectra are shown for a flow speed of 72 m/s.

Figure 4 compares the third octave spectra for the NACA 0012 and NACA 0018 airfoils installed in a configuration with a rod diameter of 10 mm and a gap of 86 mm. It can be seen that the LE noise is greater for the configuration with a NACA 0012 airfoil than for that with NACA 0018 airfoil built in. For the TE noise the dissimilarity is much smaller. According to Guidati [7] it can be assumed that the thicker NACA 0018 airfoil

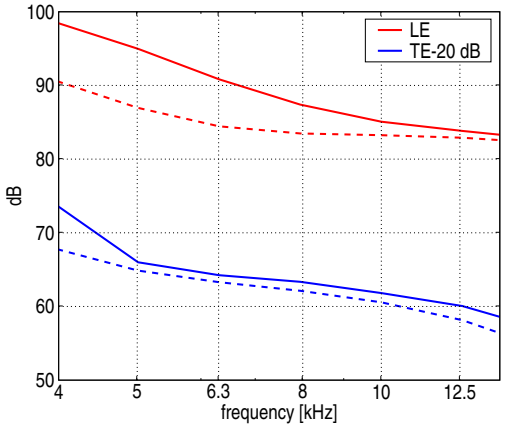

Figure 4: LE and the TE third octave spectra for the NACA 0012 (solid line) and the NACA 0018 (dashed line) airfoil for a configuration with a gap of 86 mm and a rod with 10 mm diameter.

with the bigger and blunter LE is one reason for the less LE noise generation.

The LE third octave spectra for the rod-airfoil-configuration with installed NACA 0012 airfoil are shown in Figure 5. While Figure 5a shows the curves for the configuration with a varied gap and a fix rod diameter, Figure 5b presents the spectra for the configuration with a varied rod diameter and a fix gap. The comparison of both diagrams indicates that the LE noise depends more on the rod diameter than on the gap especially for the greater rod diameters.

Figure 6 presents the curves analog to Figure 5 for the TE source. As for the LE spectra the variation of the TE noise is much less for the configurations with fix rod diameter than for that with fix gap. The comparison of the LE and TE noise for the configurations with fix gap (figures 5b and 6b) shows that the variation of the curves is greater for the LE. This is intelligible because the LE noise source is strongly influenced by the turbulence characteristic of the airfoil inflow.

Conclusion

An experimental setup for the investigation of broadband noise has been shown in detail. Further, the measuring method allowing separation of the different broadband noise sources has been explained and the analysis of the recorded acoustic data has been demonstrated. First results show that the LE noise generation is less for the configuration with NACA 0018 airfoil than for that with

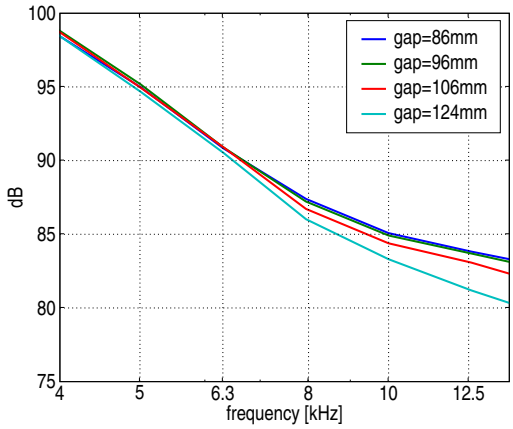

(a) fix rod diameter of 10 mm and varied gap

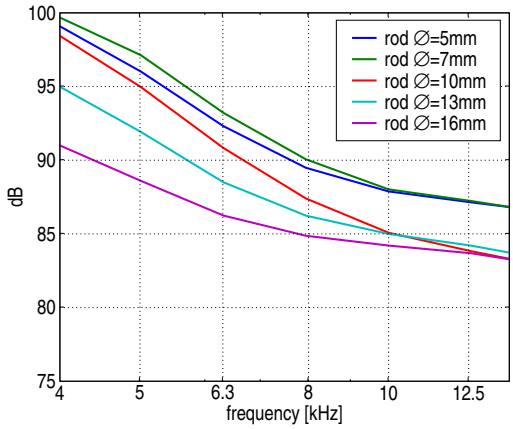

(b) fix gap of 86 mm and varied rod diameter

Figure 5: LE third octave spectra of the NACA 0012 airfoil

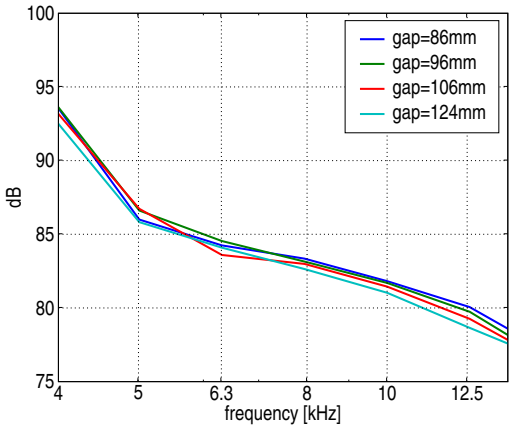

(a) fix rod diameter of 10 mm and varied gap

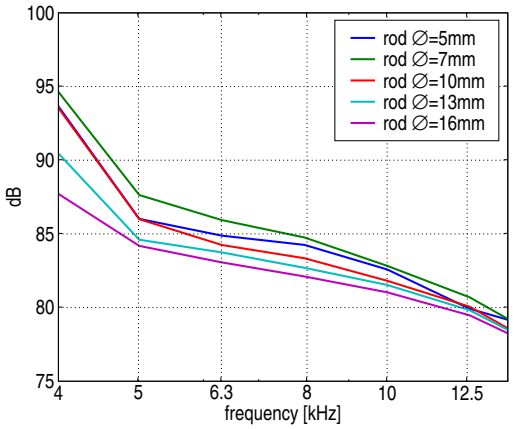

(b) fix gap of 86 mm and varied rod diameter

Figure 6: TE third octave spectra of the NACA 0012 airfoil

the NACA 0012 airfoil installed. Further, the results indicate a stronger dependence of the sound pressure level on the rod diameter than on the gap between rod and airfoil.

Acknowledgment

This work is funded by the *International Graduate School of the Brandenburg University of Technology at Cottbus* (compressor technologies and materials).

References

[1] Sarradj, E.; Windisch, T.: Konzeption und Inbetriebnahme eines aeroakustischen Freistrahl-Windkanals. *Fortschritte der Akustik - DAGA 2006.*

[2] Giesler, J.; Sarradj, E.: Modifikation am aeroakustischen Windkanal der BTU Cottbus. *Fortschritte der Akustik - DAGA 2008.*

[3] Jacob, M. C.; Boudet, J.; Casalino, D.; Michard, M.: A rod-airfoil experiment as benchmark for broadband noise modeling. *Theoret. Comput. Fluid Dynamics (2005) 19: 171-196.*

[4] Sarradj, E.: Quantitative source spectra from acoustic array measurements. In *Berlin Beamforming Conference, 2008.*

[5] Brooks, T. F.; Humphreys, W. M.: A deconvolution approach for the mapping of acoustic sources (DAMAS) determined from phased microphone arrays. *Journal of Sound and Vibration 294 (2006), 856-879.*

[6] Sarradj, E.; Geyer, T.; Giesler, J.: Aeroacoustic source characterisation using subspace and deconvolution techniques. In *Noise and Vibration: Emerging Methods, NOVEM 2009.*

[7] Guidati, G.: Berechnung und Verminderung von Strömungsgeräuschen an Profilen. *Dissertation, Universität Stuttgart, 2004.*